Vanadium Pentoxide as a hole selective contact for novel heterojunction solar cells based on n-type silicon

Luis Martín, Eloi Ros, and Raül Perea
Universitat Politècnica de Catalunya
(Supervisor: Cristóbal Voz)
(Dated: May 25, 2016)

This work reports on the use of vanadium pentoxide as a low-temperature alternative to conventional p-doped emitters for silicon solar cells based on n-type wafers. Vanadium pentoxide is a transition metal oxide, whose semiconducting properties are determined by oxygen-vacancies created during the deposition process. Due to its high work-function (> 5 eV) and wide energy band gap (> 3 eV), this transition metal oxide acts as a transparent front-side hole-selective contact. On the rear side of the n-type wafer, two different passivated back contact strategies were compared. The first one uses locally-diffused point-contacts created by laser-firing, whereas the second is based on the heterojunction with intrinsic thin layer concept. Of both rear contact types, the heterojunction performed the best with a conversion efficiency of 14.8%. These results bring into view a new silicon heterojunction solar cell concept with advantages, such as the elimination of toxic dopant gases and a more simple low-temperature fabrication process.

Keywords: Silicon heterojunction, transition metal oxide, laser-fired contact, heterojunction with intrinsic thin layer, hole-selective contact.

I. INTRODUCTION

In the last years it has been devoted a great effort to find crystalline silicon (c-Si) solar cell technologies with competitive manufacturing costs. Cost reduction strategies include using ultra-thin wafers or lower-quality substrates, but in any case lower thermal budgets and simplified fabrication processes would be desirable. In this regard, silicon heterojunction structures constitute a cornerstone where low-temperature manufacturing and high conversion efficiency can be combined. Particularly, the Heterojunction with Intrinsic Thin layer (HIT) concept combines excellent surface passivation with hole/electron-selective contacts deposited at low-temperature, achieving record efficiencies of 25.6% [1]. Nonetheless, the p/n-doped hydrogenated amorphous silicon (a-Si:H) stacks are deposited by Plasma-Enhanced Chemical Vapor Deposition (PECVD), a capital-intensive system with mandatory security systems considering the flammable and toxic boron/phosphorous gas precursors employed. In this sense, the utilization of risk-free materials deposited at low temperature is a good alternative to further decrease in production costs.

One type of materials that have demonstrated excellent carrier-selective properties are transition metal oxides (TMOs), which are wide band gap semiconductors with a distinctive p- or n-type character and a broad range of work functions varying from 2 to 7 eV [2]. Many reports can be found in the literature regarding interface engineering with TMOs applied to organic light emitting diodes (OLEDs) and organic solar cells [3], such as molybdenum trioxide (MoO_3) [4], tungsten trioxide (WO_3) [5], vanadium pentoxide (V_2O_5) [6] and rhenium trioxide (ReO_3) [7]. These TMOs work as hole-selective contacts due to their large work functions (> 5eV) laying close to the Highest Occupied Molecular Orbital (HOMO) level of several p-type organic semiconductors, which favours the formation of an ohmic contact. Thin layers of TMOs can be obtained inexpensively at low-temperature, for instance by thermal evaporation or even a solution-based process [8]. Thus, it is very motivating to explore their potential as an alternative to traditional doping processes for c-Si solar cells. However, research on the incorporation of TMOs into silicon devices dates from very recent years [9–11]. Heterojunction solar cells based on p-type c-Si with TMO layers as a rear contact were reported recently [12, 13] demonstrating low contact resistivities and efficiencies of 15%. Particularly, the use of TMOs as p-type contacts in n-type c-Si has also been investigated for MoO_3 [13–15] and WO_3 [16], demonstrating a power conversion efficiency (PCE) of 18.8% for this novel solar cell concept [17]. Recently, a comparative study between three TMOs (MoO_3, WO_3, V_2O_5) acting as hole-selective contacts in n-type c-Si solar cells reported a better performance of vanadium pentoxide [11].

In this work, the performance of V_2O_5 as a hole-selective contact on n-type c-Si is studied for two alternative low-temperature rear contacts. The first one consists in locally-diffused Laser-Fired Contacts (LFC), whereas the second one consists in a rear contact HIT.

II. EXPERIMENTAL DETAILS

A. Device Fabrication

The structures of the two different TMO/n-Si heterojunction solar cells studied in this work are depicted in Fig. 1. Two n-type Si wafers ($1.5\ \Omega \cdot$ m, 280 μm thick) were cleaned by RCA and 1% HF dipping. Both substrates were immediately loaded into a PECVD system

to deposit the corresponding stack of layers on the rear side to form the back-contact. In the LFC structure (a), this stack consisted of a 4 nm intrinsic a-SiC$_x$:H ($x \sim 0.2$) passivation layer, a 15 nm phosphorous-doped a-Si:H layer and a 80 nm a-SiC$_x$:H ($x \sim 1$) back reflector. Then, the rear side of the LFC solar cell was laser-fired to obtain an array of locally-diffused point contacts (0.5% contacted area fraction) [18]. In the HIT structure (b), the stack consisted of the same 4 nm intrinsic buffer followed by a 15 nm n-doped a-Si:H layer. In this case, the full-area rear electrode was directly an indium-tin-oxide (ITO) layer deposited by RF magnetron sputtering. After an additional 1% HF dip, the V_2O_5 (melting point 690 °C) was thermally evaporated on the front side ($\sim 8 \cdot 10^6$ mbar, ~ 0.2 Å/s). After a brief air exposure, an antireflective ITO front electrode was deposited onto the V_2O_5 layer. After lithographic patterning of 1 cm^2 active cell area, back-contact metallization was done by by thermal evaporation of aluminum and silver (1 μm) for the LFC and HIT solar cells, respectively.

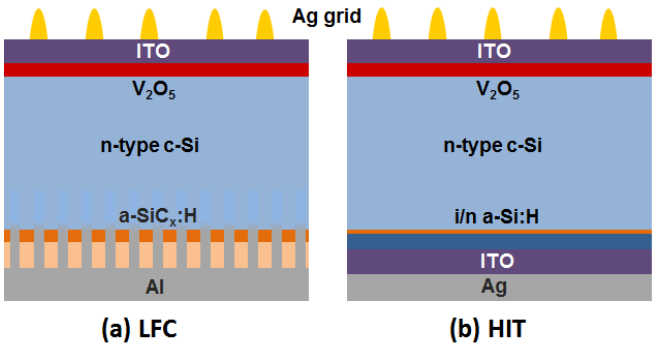

Figure 1. Schematic of the TMO/n-type c-Si solar cells studied in this work with reference LFC (a) and HIT (b) rear contact strategies.

B. Characterization Techniques

Current density–voltage (J–V) characteristics were measured in dark and under standard AM1.5 illumination (100 mWcm^{-2}) by means of a Newport Solar Simulator with a Keithley 2400 DC source-meter. Quasi-steady-state open-circuit voltage (QSSV$_{oc}$) measurements were also done in order to calculate pseudo J–V curves without the effect of the series resistance. The data extracted from QSSV$_{oc}$ were analyzed in order to calculate the effective lifetime (τ_{eff}) of the minority carriers. The effective lifetime can be written in terms of the surface recombination velocity of both front and rear surfaces:

$$\frac{1}{\tau_{eff}} = \frac{1}{\tau_b} + \frac{S_{front}}{W} + \frac{S_{rear}}{W} \quad (1)$$

where τ_b is the effective lifetime in the bulk, which results from the Shockley-Read-Hall, Auger and band-to-band recombination, and W is the thickness of the wafer. In this study, we will particularly investigate the S_{rear} values that result from the two different rear contact strategies under study: LFC and HIT.

The External Quantum Efficiency (EQE) curves of the fabricated solar cells were obtained by means of a QEX10 PV Measurements set up. The EQE is defined as the ratio between collected charge carriers and incident photons. The reflectance spectra (R) from the front side of the solar cells were measured by means of a UV-VIS-NIR Shimadzu 3600 spectrophotometer. These measurements allowed us to calculate the Internal Quantum Efficiency (IQE). The IQE is defined as the ratio between collected charge carriers and photons absorbed in the solar cell:

$$IQE(\lambda) = \frac{EQE(\lambda)}{1 - R(\lambda)} \quad (2)$$

The behaviour of the IQE at long wavelengths was analyzed to estimate the effective diffusion length (L_{eff}) of minority carriers for the fabricated solar cells [19], and thus obtain the S_{rear} value for each cell.

III. RESULTS AND DISCUSSION

A. Analysis of the Effective Lifetime

The fabricated solar cells were characterized by measuring their QSSV$_{oc}$ curves. This measurement is typically used to obtain pseudo J–V curves without the effect of the series resistance. However, QSSV$_{oc}$ data also implicitly contain information about the effective lifetime after a complete fabrication process [20].

Conceptually, τ_{eff} could be estimated from

$$\tau_{eff} \approx \frac{\Delta n}{G} \quad (3)$$

where a uniform net generation rate (G) is assumed and Δn is the average excess of minority carriers in the wafer. In good-quality solar cells, we expect a nearly flat excess carrier density in open-circuit conditions. Thus, the Δn value of equation (3) can be approximated by the excess of minority carriers at the edge of the space charge region, which can be derived from the following expression:

$$n_i^2 e^{\frac{V_{oc}}{V_T}} = np \approx \Delta n \left(N_D + \Delta n\right) \quad (4)$$

where N_D is the dopant concentration and $V_T = \frac{KT}{q}$. The solution of equation (4) for Δn is

$$\Delta n = \frac{\sqrt{N_D^2 + 4n_i^2 e^{\frac{V_{oc}}{V_T}}} - N_D}{2} \quad (5)$$

On the other hand, the value of G can be closely approximated by

$$G \approx \frac{1}{q}\frac{J_{sc}}{W} I_{suns} \tag{6}$$

where J_{sc} is the short-circuit current density and I_{suns} is the illumination intensity measured in suns, which was measured by means of a calibrated photodetector installed in the $QSSV_{oc}$ set-up. The value of J_{sc} was independently obtained from the electrical characteristic of the solar cell under AM1.5 illumination and from the EQE curve. Finally, once G and Δn have been calculated, τ_{eff} can be obtained from equation (3). The behaviour of the effective lifetime vs. minority carrier density for both solar cells with HIT and LFC rear contacts is shown in Fig. 2. The one-sun τ_{eff} value for the solar cell with HIT rear contact ($\sim$ 330 μs) is an order of magnitude larger than that of the device with a LFC rear contact ($\sim$ 50 μs). Thus, it can be affirmed that the performance of the HIT rear contact is much better than the performance of the LFC.

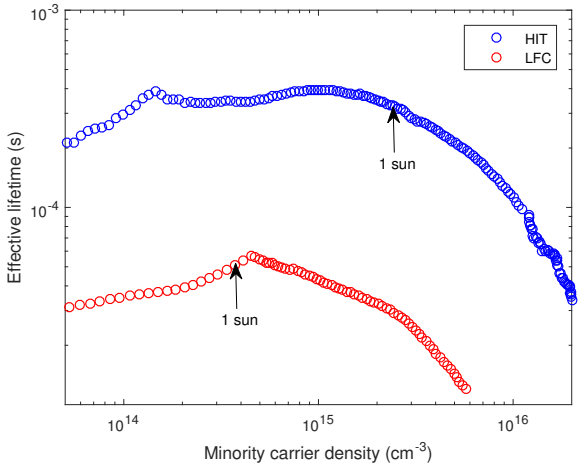

Figure 2. Effective lifetime for both HIT rear contact and LFC solar cells. The respective lifetimes for an illumination of one sun are marked with an arrow.

B. Electrical Characteristics of the Solar Cells

The J–V curves measured under standard illumination (AM1.5, 100 mW/cm^2) of the fabricated solar cells are shown in Fig. 3 for both LFC and HIT devices. Pseudo J–V curves deduced from $QSSV_{oc}$ measurements are also shown for comparison. These ideal curves, which are not affected by the series resistance, give information about the intrinsic quality of these structures. From these curves, the values of J_{sc}, V_{oc}, efficiency η, fill factor (FF) and the corresponding pseudo-parameters are extracted (see Table I). A better performance of the back-contact HIT is observed. From the pseudo-parameters, it can be deduced that both devices have a wide room for improvement by optimizing the electrodes to reduce the series resistance.

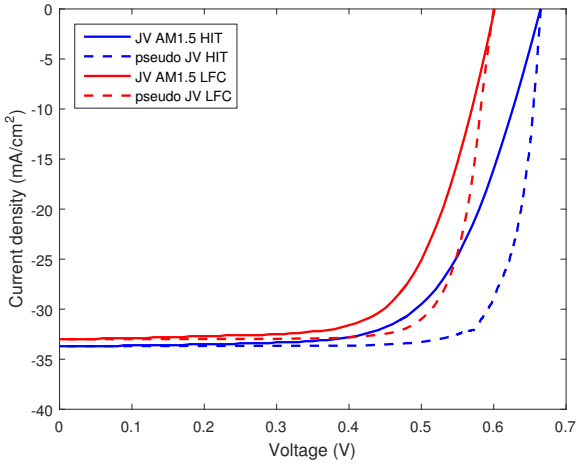

Figure 3. Current–voltage characteristics measured under AM1.5 (100 mW/cm^2) illumination (solid lines) and pseudo J–V curves (dashed lines) for both solar cells.

	HIT	LFC
J_{sc} (mA/cm^2)	33.7	33.0
V_{oc} (mV)	665	601
η (%)	14.8	13.5
FF (%)	66.3	68.0
pseudo-η (%)	18.4	15.5
pFF (%)	82.0	78.3

Table I. Summary of the parameters extracted for the electrical characterization of both LFC and HIT solar cells.

Dark J–V and pseudo J–V curves are compared in Fig. 4. The fitting to the dark J-V curves (Fig. 3) by a two-diode model leads to the values summarized in Table II [21]. The lower performance of the LFC device is mainly due to its much higher J_{01} value, which can be attributed to the rear surface recombination velocity. Besides, the R_p value was lower, which indicates the existence of pinholes derived from the fabrication process. The similarity of the other fitting parameters, particularly the series resistance, indicates that they are dominated by the front electrode based on V_2O_5.

	HIT	LFC
J_{01} (pA)	0.18	1.42
n_1	1.00	1.00
J_{02} (nA)	30	100
n_2	2.06	2.13
R_p (kΩ)	175	35
R_s (Ω)	2.1	1.9

Table II. Summary of the parameters extracted from the fitting of the dark J–V curves.

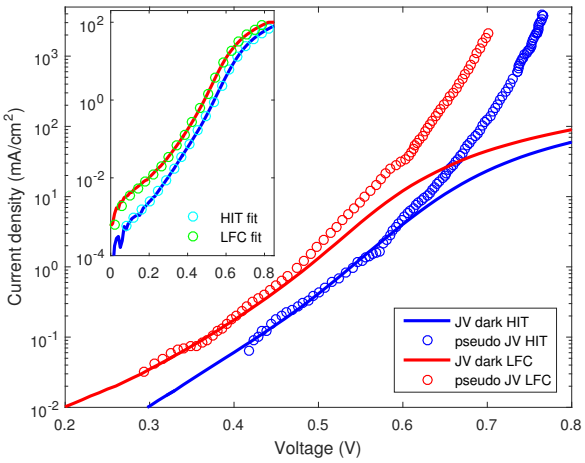

Figure 4. Current–voltage characteristics measured in dark (solid lines) and pseudo J–V curves (circles) for both solar cells. The inset shows the fitting of the J–V curves measured in dark.

C. Rear Surface Recombination Velocity

The electrical characteristics of both solar cells suggest that the back-contact HIT provides a better rear surface passivation. However, these measurements actually give information about the whole device structure. Thus, a direct estimation of the rear surface recombination velocity (S_{rear}) is necessary. This can be calculated from the IQE, which in turn is calculated from EQE and reflectance measurements (see equation (2)). The IQE of the LFC cell shows a worse behaviour in the range between 800 and 1100 nm (see Fig. 5). The IQE in this region can be fitted with the following expression [19]:

$$\frac{1}{IQE} = 1 + \frac{1}{\alpha \cdot L_{eff}} \tag{7}$$

where α is the absorption coefficient and L_{eff} is the effective diffusion length. The L_{eff} values (Table III) far exceed the wafer thickness (280 μm) for both rear structures, but it was significantly higher in the HIT device. In addition, the corresponding rear surface recombination velocity can be calculated with the following equation [22]:

$$S_{rear} = \frac{D_b}{L_b} \cdot \frac{L_b - L_{eff} \cdot \tanh\left(\frac{W}{Lb}\right)}{L_{eff} - L_b \cdot \tanh\left(\frac{W}{L_b}\right)} \tag{8}$$

where $D_b = 12\ \mathrm{cm^{-2}s^{-1}}$ is the diffusion coefficient of minority carriers in the base, and $L_b = \sqrt{D_b \tau_b} = 4900\ \mu$m is the bulk diffusion length.

The excellent S_{rear} of only 50 cm/s for the HIT device indicates a much better rear surface passivation. This result explains the higher infrared response of this device as compared to the LFC solar cell.

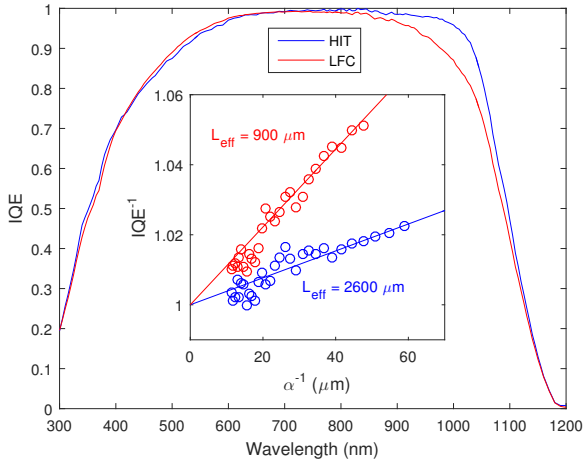

Figure 5. IQE curves of both solar cells. The insets show the inverse of the IQE vs. the penetration depth in the wavelength range from 850 to 900 nm. A linear fitting provides the values of L_{eff}

	HIT	LFC
L_{eff} (μm)	2600	900
S_{rear} (cm/s)	50	190

Table III. Summary of the calculated effective diffusion length and rear surface recombination velocity for both devices.

IV. CONCLUSION

In this work we have demonstrated the viability of V_2O_5 layers to replace conventional p-doped emitters for n-type c-Si solar cells. The V_2O_5 layers can be deposited by simple thermal evaporation, keeping the c-Si wafer at low-temperature, and circumventing the use of toxic doping gas precursors.

Two different reference rear electrodes were studied, either a LFC or a HIT structure. The last one performed much better, allowing a conversion efficiency close to 15%. These results suggest that the quality of the solar cells was limited by the rear electrode. Thus, the potential of V_2O_5 hole-selective contacts could be significantly higher.

Future work will focus on investigating alternatives for the rear electrode also based on electron-selective contacts. By doing this, a silicon-based complete solar cell could be fabricated by low-temperature process and risk-free materials, providing a progress in the development of inexpensive high-efficiency solar cells.

[1] K. Masuko, M. Shigematsu, T. Hashiguchi, D. Fujishima, M. Kai, N. Yoshimura, Y. Ichihashi, T. Mishima. N. Matsubara, et al., Achievement of more than 25% conversion efficiency with crystalline silicon heterojunction solar cell, IEEE J.Photovolt. 4, 1433–1435. (2014).

[2] J. Meyer, S. Hamwi, M. Kröger, W. Kowalsky, T. Riedl, A. Kahn, Transition metal oxides for organic electronics: energetics, device physics and applications, Adv. Mater. 24, 5408–5427 (2012).

[3] F. Wang, Z. Tan, Y. Li, Solution-processable metal oxides/chelates as electrode buffer layers for efficient and stable polymer solar cells, Energy Environ. Sci. 8, 1059–1091 (2015).

[4] H. You, Y. Dai, Z. Zhang, D. Ma, Improved performances of organic light-emitting diodes with metal oxide as anode buffer, J. Appl. Phys. 101, 026105 (2007).

[5] J. Meyer, S. Hamwi, T. Bülow, H.H. Johannes, T. Riedl, W. Kowalsky, Highly efficient simplified organic light emitting diodes, Appl. Phys. Lett. 91, 113506 (2007).

[6] G. Li, C.W. Chu, V. Shrotriya, J. Huang, Y. Yang, Efficient inverted polymer solar cells, Appl. Phys. Lett. 88, 253503 (2006).

[7] D.S. Leem, H.D. Park, J. W Kang, J.H. Lee, J.W. Kim, J.J Kim, Low driving voltage and high stability organic light-emitting diodes with rhenium oxide-doped hole transporting layer, Appl. Phys. Lett. 91, 011113 (2007).

[8] J. Meyer, R. Khalandovsky, P. Görrn, A. Kahn, MoO_3 Films Spin-Coated from a Nanoparticle Suspension for Efficient Hole-Injection in Organic Electronics, Adv. Mater. 23, 70–73 (2011).

[9] S.I. Park, S.J. Baik, J.S. Im, L. Fang, J.W. Jeon, K.S. Lim, Towards a high efficiency amorphous silicon solar cell using molybdenum oxide as a window layer instead of conventional p-type amorphous silicon carbide, Appl. Phys. Lett. 99, 063504 (2011).

[10] J.H. Yang, S.J. Kang, Y. Hong, K.S. Lim, Doping-free intrinsic amorphous silicon thin-film solar cell having a simple structure of glass/SnO_2/MoO_3/i-a-Si/LiF/Al, IEEE Electron Device Letters 35, 96-98 (2014).

[11] L.G. Gerling, S. Mahato, A. Morales-Vilches, G. Masmitja, P. Ortega, C. Voz, R. Alcubilla, J. Puigdollers. Transition metal oxides as hole-selective contacts in silicon heterojunctions solar cells. Solar Energy Materials and Solar Cells 145, 109-115 (2016).

[12] A. Morales, L.G. Gerling, J. Puigdollers, C. Voz, R. Alcubilla, Doping-free alternatives for passivated back contacts in silicon heterojunction solar cells, (MRS, San Francisco, CA, 2015) Materials Research Society. Spring Meeting & Exhibit.

[13] J. Bullock, A. Cuevas, T. Allen, C. Battaglia, Molybdenum oxide MoO_x: a versatile hole contact for silicon solar cells, Appl. Phys. Lett. 105, 232109 (2014).

[14] C. Battaglia, X.Yin, M. Zheng, I.D. Sharp, T. Chen, S. McDonello, A. Azcatio, C. Carraro, B. Ma, R. Maboudian, et al., Hole selective MoO_3 contact for silicon solar cells, Nano Lett. 14, 967-971 (2014).

[15] L. Ding, M. Boccard, Z. Holman, and M. Bertoni, Evaluation of transition metal oxides as carrier-selective contacts for silicon heterojunction solar cells, (MRS, San Francisco, CA, 2015) Materials Research Society. Spring Meeting & Exhibit.

[16] M. Bivour, J. Temmler, H. Steinkemper, M. Hermle, Molybdenum and tungsten oxide: High work function wide band gap contact materials for hole selective contacts of silicon solar cells, Solar Energy Materials and Solar Cells 142, 34-41 (2015).

[17] C. Battaglia, S.M. de Nicolás, S.D. Wolf, X. Yin, M. Zheng, C. Ballif,A. Javey, Silicon heterojunction solar cell with passivated hole selective MoO_x contact, Appl. Phys. Lett. 104, 113902 (2014).

[18] M. Colina, A. B. Morales-Vilches, C. Voz, I. Martin, P.R. Ortega, R. Alcubilla, Low surface recombination in silicon-heterojunction solar cells with rear laser-fired contacts from aluminum foils, IEEE J. Photovolt. 5, 805–811 (2015).

[19] P.A. Basore, Extended spectral analysis of internal quantum efficiency, (IEEE, Lousville, KY, 1993) Photovoltaic Specialists Conference, Conference Record of the Twenty-Third IEEE, pp. 147-152

[20] M.J. Kerr, A. Cuevas, and R.A. Sinton, Generalized analysis of quasi-steady-state and transient decay open circuit voltage measurements, J. Appl. Phys. 91, 399 (2002).

[21] A. Hovinen, Fitting of the solar cell IV-curve to the two diode model, Physica Scripta T54, 175 (1994).

[22] M. Spiegel, B. Fischer, S. Keller, E. Bucher, Separation of bulk diffusion length and back surface recombination velocity by improved IQE-analysis, (IEEE, Anchorage, AK, 2000) Photovoltaic Specialists Conference, Conference Record of the Twenty-Eighth IEEE, pp.311–314.